Journal of Nuclear Materials 396 (2010) 257–263

Contents lists available at ScienceDirect

Journal of Nuclear Materials

journal homepage: www.elsevier.com/locate/jnucmat

Nanosecond laser ablation of Thoria fuel pellets for microstructural study

Sucharita Sinha *

Laser and Plasma Technology Division, Bhabha Atomic Research Centre, Trombay, Mumbai 400 085, India

A R T I C L E I N F O

Article history:
Received 23 July 2008
Accepted 22 November 2009

A B S T R A C T

A two-dimensional numerical model has been developed simulating the process of laser based surface etching of Thoria targets via pulsed laser ablation enabling their surface preparation for subsequent metallographic investigation. The heat conduction equation solved by an explicit finite difference method provides simulated data on the temperature distribution at the surface and within the target, melt depth and evaporation rate from the target as a function of time, during and after the laser pulse. Calculations have been performed for laser and target parameters corresponding to experimental conditions matching our reported experimental observations on pulsed laser etching of Thoria pellets via laser ablation. The calculated maximum surface temperature reached by the laser treated Thoria target exceeds the estimated value of thermodynamic critical temperature of Thoria. Thus, our results on simulation of pulsed laser ablation for an average laser flux of 10 J/cm^2 delivered by a 10 ns Nd:YAG laser pulse corresponding to a peak laser intensity of 3.87×10^9 W/cm^2 suggest, that explosive boiling could probably be an additional material-removal mechanism other than normal boiling and evaporation when surface etching Thoria with such intense laser radiation. Since explosive boiling is usually accompanied by intense material ejection, this mechanism of material-removal should be avoided to ensure minimum induced target damage associated with the technique of laser based etching. Our calculations thus help us to make a proper choice of laser parameters facilitating subsequent metallographic investigation of laser etched Thoria fuel pellets, at the same time, minimizing unwanted associated thermal effects such as target damage through crater formation, as has been experimentally observed.

1. Introduction

Fuel used for nuclear reactors are usually in the form of ceramic oxide pellets [1]. When exposed to the high temperatures, high temperature gradients, fission products and high radiation levels within the reactor, both fuel and cladding material are likely to undergo complex thermal and chemical changes. Thus, structural integrity of these fuel pellets as well as that of their clad material is highly susceptible to damage given the extreme conditions to which these fuel elements are subjected inside the reactor. In fact, irradiation damage and thermal stress have been observed to result in extensive environment assisted cracks within the fuel-clad structure [2,3]. Therefore, periodic inspection and post irradiation examination of spent nuclear fuel, aimed towards evaluating and improving the performance and safety of the nuclear reactor, need to be carried out on a regular basis.

Metallographic investigation of the irradiated fuel pellets typically inspects the granular microstructure, grain boundaries and extent of porosity within these irradiated fuel pellets. Such metallographic investigation require prior surface preparation of these pellets involving the process of surface etching which reveals the microstructure and the grain boundaries in the solid fuel elements. Since irradiated fuel pellets often develop cracks vacuum impregnation of the fuel element sections with an epoxy compound becomes necessary that fixes the cracked fuel pieces together holding them in position prior to metallographic investigations. In case of irradiated Thoria pellets conventional etching techniques such as thermal etching or chemical etching methods [4–6] affect this binding epoxy compound resulting in disintegration of the Thoria pellet. Therefore, both these etching techniques prove to be inappropriate for surface preparation of irradiated Thoria pellets. However, recently laser based etching has been reported as a potential alternative etching technique that has successfully revealed the microstructure of Thoria fuel elements thus enabling their subsequent metallographic investigation [7]. This laser based etching technique permits strongly localized heat or photo-treatment of materials and thus has several advantages as compared to conventional etching techniques. It does not involve use of chemical reactants, thereby minimizing waste generation. In addition, it benefits enormously from the typical characteristics of laser radiation, namely, remote processing capability, excellent spatial and temporal resolution of etched surface on account of high intensity and directionality of the processing laser beam. Etching rates with lasers strongly depend on the microstructure and morphology of the material and its optical and thermal properties, in

* Tel.: +91 22 25595352; fax: +91 22 25505151/+91 22 25519613.
E-mail address: ssinha@barc.gov.in

0022-3115/$ - see front matter © 2009 Elsevier B.V. All rights reserved.
doi:10.1016/j.jnucmat.2009.11.019

addition to laser parameters such as irradiance, pulse duration, pulse repetition frequency and laser wavelength.

Primary interaction between light and matter occur through non-thermal energy coupling either via elementary excitations in the medium that are optically active or through localized or non-localized electronic or vibrational excitations that are related to defects, impurities or to the solid surface [8]. Depending on the extent of electron–phonon coupling in the solid this absorbed energy gets transferred, thereafter, to the lattice, leading to strong lattice vibrations within the solid, heating and subsequent thermal ablation from the etched surface. Although, laser based etching can occur both, due to thermal and non-thermal ablation, ablation induced by laser pulses of nanosecond or longer pulse duration are largely thermal in nature. Significant surface etching via pulsed laser ablation has been observed to occur only if the laser fluence exceeds a certain threshold value φ^{th}, that strongly depends on the material being etched and also the laser parameters. Another major advantage typical of pulsed laser ablation is associated with minimum dissipation of energy beyond the volume being ablated during the pulse, and this limits the heat affected zone and associated collateral damage. Typically, this condition is fulfilled if the thickness of the layer ablated per laser pulse is of the order of the heat penetration depth, or the optical penetration depth, whichever is larger. In order to achieve an optimum quality of etching of Thoria samples via laser ablation thereby successfully revealing their microstructure with good reproducibility, and with minimum associated target damage, the ablation mechanism needs to be well understood.

Laser ablation is a technique having potential, as well as, established applications in a wide range of scientific and industrial areas. These include pulsed laser deposition and thin film generation, surface treatment, micromachining, clusters and nanoparticle formation, medical applications, as also use of laser ablation in several analytical techniques where this technique is used for both, sample preparation and analysis [8,9]. However, in spite of the many applications, the exact mechanism of laser ablation remains yet to be fully understood. This happens largely due to the fact that the actual mechanism through which laser energy gets coupled and subsequently dissipated in the target medium differs for different application processes, depending on the type of material being processed, operation parameters of the processing laser and also the prevailing ambient conditions. As identification and understanding of the relevant material-removal mechanism is the key to accurately estimating ablation rates for a given laser irradiance, there exists a need to develop an appropriate theoretical model for the process that can reliably predict the application technique.

Several experimental observations over the years have provided valuable insights into the fundamental processes involved in laser ablation and a variety of theoretical models have been proposed explaining these experimental observations [10–17]. The process of laser ablation broadly consists of deposition of energy into the material, subsequent modification of the material induced by the laser pulse and finally the features of the ablated vapor including plasma formation, in case of processing being done using an intense enough laser beam. Depending on the laser irradiance, material removal occurs either in the form of fine vapor, liquid droplets or even solid flakes and fragments [8]. In order to describe these complex mass removal mechanisms via laser ablation, it is necessary to know the extent of absorption of laser radiation in the target, resultant heating of the solid target leading to ablation of the target material either through normal vaporization, boiling or under super-heated condition of the target when material removal occurs through hydrodynamic instability and explosive boiling, largely when high fluence laser pulses are utilized [16,18].

We report here, our efforts towards development of a numerical model describing the process involved in laser based etching of Thoria via pulsed laser ablation. This, to the best of our knowledge, is the first report on theoretical simulation of laser ablation of Thoria. In keeping with our experimental observations related to the specific application of laser based surface preparation of Thoria pellets for metallographic investigations [7], we have considered the particular case where a nanosecond pulsed laser is utilized to laser ablate Thoria fuel pellets. Through this simulation model we seek to develop an understanding of the process of laser based etching of Thoria and make theoretical estimates of process features such as time evolution of temperature distribution in the target, melt depth and ablation rates. Such a simulation study would enable us to judiciously choose laser operating parameters optimizing the process of laser etching, ensuring at the same time a minimum heat loading and laser induced damage to the Thoria target. Given the fact that very few reports exist in literature enumerating the material physical properties of Thoria such as its optical and thermal properties, we have started with a simple model for laser ablation of Thoria in vacuum using a nanosecond laser utilizing the limited available data on Thoria.

2. Theoretical model

2.1. Model description

When a high power laser beam is incident on a target, the target absorbs the laser energy, gets heated and vaporizes. If the vapor formed is significantly energized on absorbing the incident laser beam it can subsequently be ionized leading to plasma formation. Therefore, interaction of high-intensity laser pulse with a target surface is quite a complex physical process involving laser-surface interactions at the target and plasma formation. We have however, for the sake of simplicity, neglected ionization of vapor and plasma formation in the simulation being presented here. Or in other words, the vapor plume has been assumed to be optically thin, thereby implying that absorption of the incident laser beam in the ejected plume is negligible. Along with vapor cloud formation on laser induced heating of a solid target there could also occur a reverse flow of vapor from the cloud back to the target surface owing to collisions of particles within the cloud. However, this back flux of vapor, whose magnitude varies from zero for a collision-less expansion to a value corresponding to stationary expansion into vacuum, has been neglected in our model [8].

When the laser beam is focused on the solid target, a fraction of the laser radiation gets reflected or scattered, while, the remaining gets absorbed by the target resulting in heating of the target followed by melting and evaporation. This description of the laser-solid interaction is essentially on a macroscopic scale and involves the thermal heat conduction equation. The process by which laser energy gets coupled into the target medium varies depending on the laser pulse duration and the nature of the target medium. For nanosecond pulsed laser interaction with the target, optical energy deposited in the medium can be regarded as being instantaneously turned into heat, largely because of rapid energy relaxation from the excited electrons in the solid target to the target lattice phonons, which typically occurs on time scales of a few 100 ps [19]. However, for picosecond and femtosecond laser pulses, electron energy cannot be regarded to instantaneously convert into heat and in that case, a two-temperature model is usually considered to describe the coupling of the electron temperature and the lattice temperature [20].

Assuming an ablation process that is purely thermal in origin, ablation can occur via vaporization or explosive boiling in the time scale of nanosecond pulse duration of processing laser. However, explosive boiling only occurs when the target temperature near the critical temperature values are reached for the solid material [21–23]. For temperatures distinctly lower than this critical temperature ablation mechanism is primarily via vaporization.

Once, laser energy has been deposited into the target, the resultant distribution in temperature T, in the absence of convective and radiative energy transport, is described by the heat conduction equation, which in two dimension is written as:

$$\rho(T)C_p(T)\delta T(x,z,t)/\delta t = \nabla[\kappa(T)\nabla T(x,z,t)] + Q(x,z,t) \quad (1)$$

Table 1
Parameters for ThO_2 – input data used for our model.

Parameters	Values for ThO_2	Refs.
Thermal conductivity, κ ($W\,cm^{-1}\,K^{-1}$)	0.06 (at 500 K) 0.03 (at 1000 K)	[25,28]
Specific heat, C_p ($J\,gm^{-1}\,K^{-1}$)	0.23 (at 300 K) 0.3349 (at 1000 K)	[25,28]
Mass density, ρ ($gm\,cm^{-3}$)	9.8	[25,28]
Absorption coefficient, α (cm^{-1})	1.4226×10^4	[24,29,30]
Reflectivity used in model, R	0.5	[24,29]
Melting point, T_m (K)	3493	[25,28]
Boiling point, T_b (K)	4673	[25,28]
Heat of fusion, ΔH_{sl} ($J\,g\,m^{-1}$)	0.398×10^3	[25]
Heat of vaporization, ΔH_{lv} ($J\,g\,m^{-1}$)	2.108×10^3	[25]

Table 2
Laser parameters – input data for our model.

Nd:YAG laser parameters	Value
Wavelength, λ (nm)	532
Pulse temporal profile, and pulse duration – full width at half maximum, FWHM (ns)	Gaussian, FWHM = 5
Pulse peak, t_0 (ns)	20
Spatial profile – FWHM (μm)	Gaussian, FWHM = 420

where x and z are space coordinates, z depicting depth, i.e., spatial coordinate in the direction normal to the target surface while, x denotes space coordinate in the transverse plane. ρ, C_p and κ are mass density, specific heat at constant pressure, and thermal conductivity of the target material. The first term on the right hand side of above equation represents heat conduction, while the source term denoted by $Q(x, z, t)$ represents the laser energy absorbed by the target sample. This is expressed as:

$$Q(x,z,t) = I_S(x,t)(1\text{-}R)\alpha\exp(-\alpha z) \quad (2)$$

where R and α are the reflectivity and the absorption coefficient of the target surface and bulk material at the incident radiation wavelength characterizing the processing laser. $I_S(x, t)$ denotes the instantaneous laser irradiance at the sample surface determined by the temporal and spatial profile of the incident laser pulse. For our experimental laser surface etching system a pulsed Nd:YAG laser operating at its second harmonic wavelength of 532 nm has been employed [7]. The temporal profile of the laser pulse is typically depicted by a Gaussian in time having a full width at half maxima (FWHM) of 5 ns.

Pulsed laser ablation with short laser pulses permits suppression of heat dissipation beyond the volume being ablated. Optical penetration depth or absorption length of laser radiation in the target is defined by $l_{abs} = 1/\alpha$ [8] where α is the absorption coefficient of laser radiation within the target material. In case of Thoria, l_{abs} is typically of the order of 0.7 μm [24]. The thermal diffusion length in Thoria defined by $l_{th} \sim 2(D\tau_L)^{1/2}$, where D is the heat diffusivity of the target material defined by $D = \kappa/\rho Cp$, τ_L is the laser pulse duration [8], and this in case of Thoria lies in the region of 0.28 μm [25]. Since, both these characteristic lengths that determine the volume of interest within the target, are much smaller than the typical laser beam diameter (700 μm) irradiating the target surface being processed, lateral heat flow can be ignored and the heat conduction equation can be broadly solved in one dimension in space, i.e., the depth dimension.

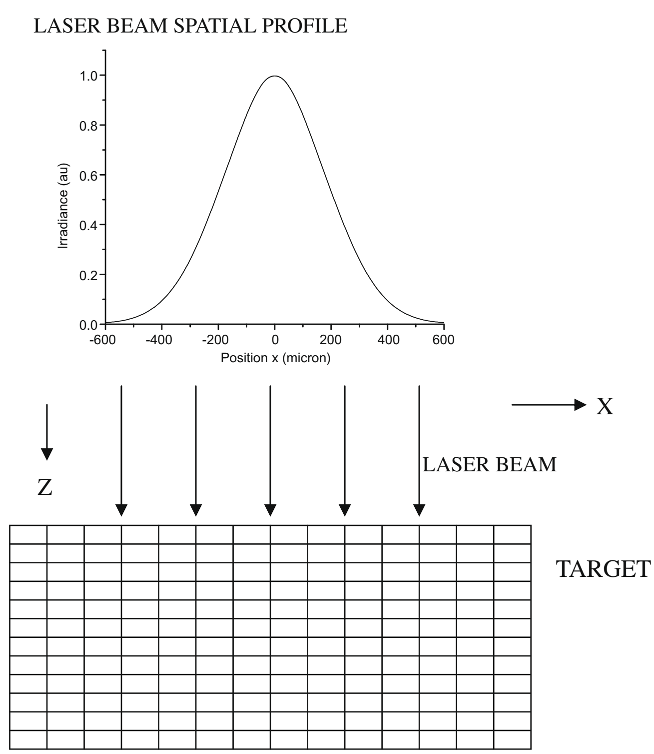

Fig. 1. Geometry for laser ablation of Thoria target.

In our experimental set-up, the laser beam utilized for laser etching of Thoria has a spatial distribution of irradiance in the transverse direction, within the laser spot. This is represented by a Gaussian distribution in a plane transverse to the direction of propagation of the laser beam. The spatial variation in irradiance distribution results in variation of the source term Q across the transverse plane, and this has been accounted for in our simulation model by dividing the transverse plane into several concentric rings with each annular region having an appropriate source term $I_S(x, t)$.

2.2. Explicit finite difference method

In order to simulate ablation of Thoria, the heat conduction equation (1) is solved as a function of time during and after the laser pulse by an explicit finite difference technique. Solving the heat conduction equation determines temperature T reached at various positions on the target surface as also within its bulk at various time instants due to energy deposited by the processing laser in the target material. The target, for this purpose is represented by a mesh of finite elements that are subject to change with time to account for simulation of material removal.

When the temperature at a certain depth in the target exceeds the melting point of Thoria, the target begins to melt, the local temperature remaining constant while phase transition takes place. Heating of molten Thoria is calculated using data on molten Thoria, wherever available [25]. In molten phase, convection is usually induced by the presence of a thermal gradient. Although, this effect leads to an additional heat transport mechanism, for simplicity we have neglected convection in our model. Melting begins on the surface of the target and the melt front gradually moves into the target depth as the temperature inside the target rises and exceeds the melting point.

The initial temperature all over and within the target is assumed to be 300 K. If the temperature of a mesh element exceeds the melting temperature of Thoria at the end of a particular time step, melting is assumed to have occurred and latent heat of fusion or heat of melting (ΔH_{sl}) is taken into account in the following calculation time steps. Similarly, when the temperature of the surface elements is comparable to the boiling temperature of the target material, substantial ablation is assumed to occur. When this happens an ablation depth h is estimated and compared with the element thickness, Δz. If $h > \Delta z$, the element is assumed to have vaporized and the surface temperature of the remaining target is accordingly corrected taking into account the latent heat of vaporization.

When temperature at the surface becomes higher than the boiling point significant vaporization of the target occurs. The vapor pressure (p_{vap}) of the ablated vapor is calculated from the surface temperature, by integrating the Clausius–Clapeyron equation [8],

$$p_{vap}[T_s] = p_0 \exp[\Delta H_{1v}(T_s - T_b)/RT_sT_b] \tag{3}$$

where T_s and T_b are the surface temperature and the normal boiling point at pressure p_0 = 1 atm, ΔH_{lv} is the latent heat of vaporization, and R is the gas constant.

Having calculated the vapor pressure p_{vap}, vapor density at the surface ($\rho_{vap,s}$) is calculated assuming the ideal gas law:

$$\rho_{vap,s} = p_{vap}/K_BT_s \tag{4}$$

where K_B is the Boltzmann constant.

Assuming that the vapor atoms leaving the surface obey a one-dimensional Maxwellian velocity distribution, the flow velocity of vapor atoms above the ablated target surface ($\upsilon_{vap,s}$) can be approximated by the average of the normal velocity component at temperature T_S [26],

$$(\upsilon_{vap,s}) = [2K_BT_S/\pi m]^{1/2} \tag{5}$$

where m is the mass of a Thoria molecule. The flow of material vaporized from the surface resulting in ablation is estimated using Eqs. (3)–(5).

2.3. Laser and target parameters – inputs for simulation

Of the incident laser irradiance on the Thoria target surface, a fraction is reflected while, the remaining irradiance is gradually absorbed in the target, the penetration depth of laser radiation in the target material being determined by the absorption coefficient of laser radiation in the target. At the start of laser processing of the target, the extent of laser radiation that is scattered away by the target surface can be reduced by suitably polishing the surface. However, this scattered component can increase rapidly during laser ablation. This is attributed to surface roughening due to the increased surface temperature resulting in surface melting and removal of surface layers [8,27]. However, in the absence of accurate estimates for the varying value of surface reflectivity of the target Thoria pellets being laser etched, we have used a constant value of 0.5 for surface reflectivity.

All physical parameters used as input data in the model are presented in Tables 1 and 2. In our model, nonlinearities in material

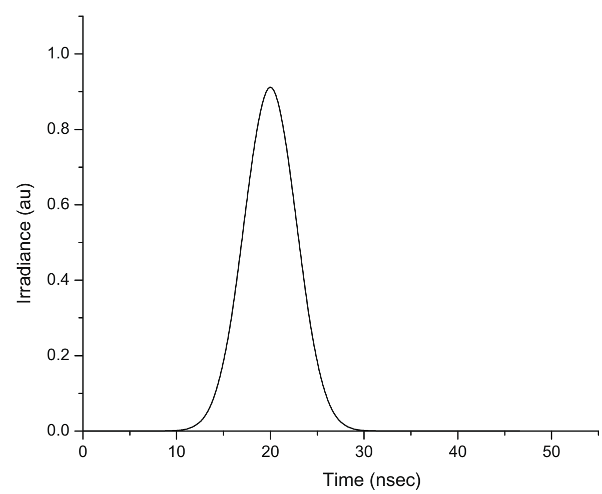

Fig. 2. Temporal profile of the incident laser pulse used for etching of Thoria.

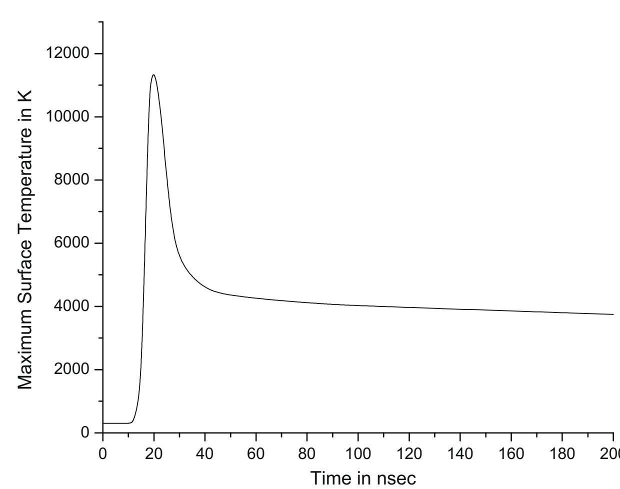

Fig. 3. Calculated temporal evolution of peak temperature at laser treated Thoria target surface for an incident peak laser intensity of 3.87×10^9 W/cm^2 and average laser flux of 10 J/cm^2.

parameters such as absorption coefficient have been neglected and the thermal properties of the target material have been assumed to be temperature dependent only in the temperature range for which data on temperature dependence of physical parameters for ThO_2 are available in literature [25].

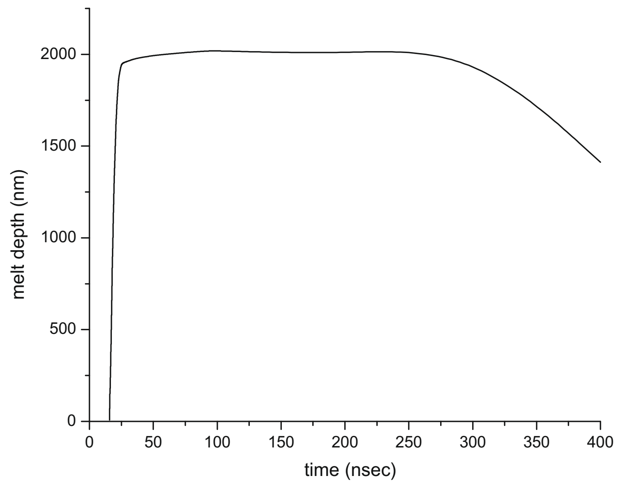

Fig. 4. Calculated variation of melt depth in laser treated Thoria target during and after the laser pulse for average incident laser flux of 10 J/cm^2.

The geometry used for simulation being reported in this work is illustrated in Fig. 1. Owing to the axial symmetry of the problem and in order to minimize computer processing time, temperature in the processed region of the target is simulated only over one half of the target in the transverse plane. Thus simulation is done over a total target volume extending to 3 μm in depth and 600 μm in transverse or radial dimension with respect to the axis of the propagating laser beam. The size of the mesh in the depth dimension was taken to be 4 nm corresponding to a time step of 1 ps to comply with the stability condition associated with the explicit finite difference technique employed in this simulation. The mesh dimension in the transverse direction was chosen to be 10 μm to account for the Gaussian nature of the spatial profile of the incident laser beam.

The reflectivity (R) and absorption coefficient α for Thoria were calculated from the real and imaginary parts of the refractive index n and k from Refs. [24,29,30] and using the following equations:

$$\alpha = 4\pi k/\lambda, \text{ and } R = \{(n-1)^2 + k^2\}/\{(n=1)^2 + k^2\}$$

where λ is the wavelength of the incident laser.

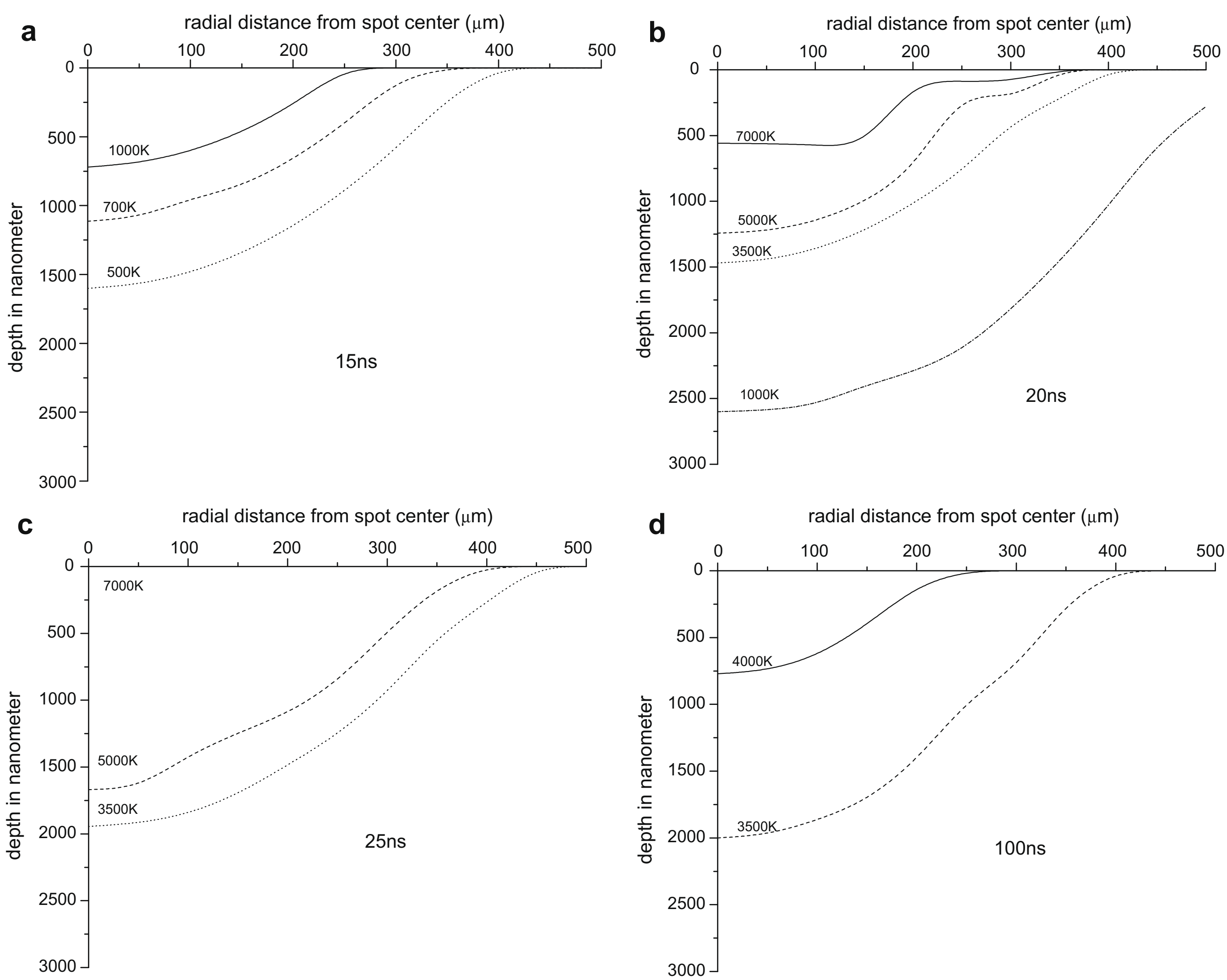

Fig. 5. Calculated temperature distribution in the Thoria target at varying depths as a function of time: (a) 15 ns, (b) 20 ns, (c) 25 ns, (d) 100 ns, processed with Nd:YAG laser radiation at 532 nm and peak intensity of 3.87×10^9 W/cm^2.

The latent heat of fusion or melting and the latent heat of vaporization of Thoria has been obtained from Refs. [25] and [28] which also provides ΔH_{sl} and ΔH_{lv} as a function of temperature.

3. Results and discussion

Solution of the heat equation gives estimates of the temperature distribution within the laser treated target at various time instants. The calculations were performed for a Gaussian shaped laser pulse having a full width at half maximum of 5 ns and peak laser irradiance of 3.87×10^9 W/cm^2 at 20 ns (Fig. 2). Intensity distribution in the transverse plane within the focused laser spot is also closely depicted by a Gaussian distribution having a full width at half maximum of 420 μm. When time and space integrated over the entire laser pulse, these laser parameters yield an average fluence of 10 J/cm^2 in the focused laser beam. The laser wavelength was taken to be 532 nm corresponding to the second harmonic emission from a Nd:YAG laser. Our experimental observations on laser etching of Thoria used a single shot of laser pulse [7]. Hence calculations reported here have been carried out for laser based etching using a single laser pulse.

Simulation results showing the temporal evolution of the maximum temperature at the surface of the target being etched is depicted in Fig. 3, which depicts the peak temperature attained at the center of the irradiated spot on the Thoria surface during and after the laser pulse. With the incident laser pulse depositing energy to the target the temperature at its surface increases with a time constant that is largely determined by the material thermal parameters such as conductivity, and specific heat as well as optical properties such as absorption coefficient and surface reflectivity of target at the incident laser wavelength. In the absence of ablation, at the end of the laser pulse the target surface temperature is expected to gradually drop with heat being conducted away from the surface into the bulk of the target at a characteristic rate. However, when laser induced ablation occurs, both latent heat of melting and evaporation is provided by the laser heated target, thus resulting in a rapid drop in surface temperature at the end of the laser pulse.

In Fig. 4 is shown the time evolution of the maximum melt depth in the target as the laser pulse deposits energy into it. During the initial stages the maximum melt depth increases rapidly closely following the rising edge of the laser pulse. Thereafter, the maximum melt depth is maintained at a nearly constant value even when the laser pulse is long over. The energy deposited and stored within the irradiated volume of target is gradually dissipated into the bulk, largely through conduction, which is rather slow in this case owing to the poor conductivity value of the target.

If energy stored within the irradiated volume of the target is large, melting and ablation may continue for a certain interval of time much after the laser pulse is over. After the end of the laser pulse only that part of the target whose temperature is high enough will ablate. The layer thickness ablated per laser pulse depends largely on the particular material under investigation, laser pulse duration and the laser fluence φ. Typically, dissipation of energy by heat conduction is characterized by the time $t_T \sim z_0^2/4D$ and the process of ablation is characterized by a time $t_A \sim z_0/v_{st}$, where z_0 is the typical thickness of the overheated layer of the target material, D is the diffusivity of the material and v_{st} is the velocity of the evaporation front. When $t_T > t_A$ a layer of thickness z_0 may be ablated even after the laser pulse is over [8].

Temperature distribution in the laser treated target as a function of time during and after the laser pulse was obtained along the radial direction at various depth values within the target. These are depicted in Fig. 5. At 15 ns the surface temperature of the target (2000 K) is lower than the melting temperature of ThO_2 thus no molten pool is generated. At 20 ns the peak surface temperature of the target rises to 11,500 K (Fig. 3) resulting in considerable ablation and material removal from the etched surface. Along with ablation a fraction of energy is removed as latent heat of vaporization. Thus the temperature drops substantially and at 25 ns the temperature distribution in the target at varying depths (Fig. 5c) reflects this effect with peak surface temperature falling to 8000 K at 25 ns (Fig. 3). The maximum ablation depth (about 2 μm) is reached at around 40 ns. Beyond 40 ns when the laser pulse is almost over, the temperature of the laser irradiated region falls gradually, reaching a peak surface temperature slightly exceeding 4000 K at 100 ns. The temperature in this time range continues to decrease mainly due to conduction of heat into the bulk of the target material.

During pulsed laser ablation of solids, three mechanisms are generally observed that are of thermal origin: normal vaporization, normal boiling and explosive boiling (phase explosion) [18,21]. For nanosecond laser pulses, the regime of normal vaporization leads

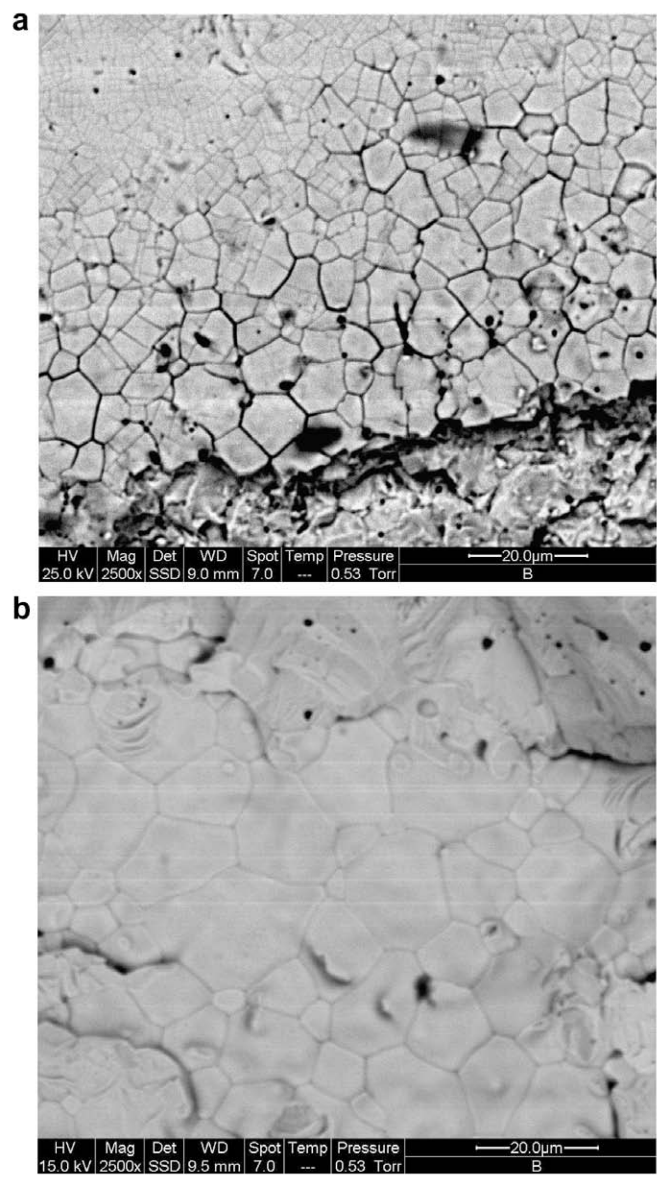

Fig. 6. Laser etched Thoria pellet: (a) SEM image showing damaged regions evident in the lower part of the image that have been subjected to intense laser radiation owing to presence of hotspots in laser beam; (b) SEM image of nanosecond laser etched Thoria surface showing good quality surface etching and clearly revealing grain structure.

to phase explosion with increasing laser fluence when the irradiated matter approaches the thermodynamic critical point, i.e., when the target temperature reaches temperatures near the thermodynamic critical values of the material [22]. Although, our model assumes a purely vaporization based material ablation, occurrence of explosive boiling at extreme temperatures is also a possibility. A large increase in ablation rate accompanied by ejection of droplets and fragments generally indicates onset of explosive boiling [18,21]. In order to determine whether explosive boiling could also contribute to material removal during the process of laser based etching of Thoria, the critical temperature of ThO_2 needs to be estimated first. In the absence of reported data on measured critical temperature of ThO_2, we used estimates of the thermodynamic critical temperature for ThO_2 using empirical equations based on the boiling temperature and the latent heat of vaporization [23]. The critical temperature for ThO_2 estimated using these empirical equations was found to range between 9500 K and 10,500 K. The maximum temperature reached by the laser irradiated surface of ThO_2 as calculated by our theoretical model for a peak incident laser intensity of 3.87×10^9 W/cm^2 corresponding to a time and space averaged laser flux of 10 J/cm^2 is of the same order as the estimated critical temperature. Thus, material-removal through explosive boiling could be a plausible mechanism during the process of pulsed laser based surface etching of Thoria. This is also evident from our experimental observations shown in Fig. 6a where target damage through crater formation in localized regions of the laser irradiated surface of Thoria fuel pellets are clearly visible in the lower region of the picture. Since explosive boiling usually results in intense ejection of target material, this mechanism should be avoided by suitably limiting the incident laser intensity levels used for the etching of Thoria elements. This would ensure good optical quality etched Thoria surface (a typical experimental observation made by us is shown in Fig. 6b achieved using a nanosecond Nd:YAG laser) with minimum laser induced damage associated with the technique of laser based etching.

4. Conclusion

A two-dimensional numerical model has been developed simulating the process of laser based surface etching of Thoria targets via pulsed laser ablation. The heat conduction equation solved by an explicit finite difference method provides the temperature distribution at the surface and within the target, melt depth and evaporation rate from the target as a function of time, during and after the laser pulse. Our results on simulation of pulsed laser ablation performed for an average laser flux of 10 J/cm^2 delivered by a 10 ns Nd:YAG laser pulse suggest, that explosive boiling could probably be an additional material-removal mechanism other than normal boiling and evaporation when surface etching Thoria with such intense laser radiation. Since explosive boiling is usually accompanied by intense material ejection, this mechanism should be avoided in order to ensure minimum induced target damage associated with the technique of laser based etching and surface preparation of Thoria fuel pellets for subsequent metallographic investigations. Our calculations thus help us to make a proper choice of laser parameters enabling metallographic investigation of laser etched Thoria fuel pellets with minimum unwanted associated thermal effects such as redeposited debris and target damage through crater formation as has been experimentally observed.

References

[1] K.D. Reeve, Ceramurgia International 1 (2) (1975) 59.
[2] M. Stan, J.C. Ramirez, P. Cristea, S.Y. Hu, C. Deo, B.P. Ubernaga, S. Srivilliputhur, S.P. Rudin, J.M. Wills, J. Alloys Compd. 444–445 (2007) 415.
[3] L. Desgranges, Ch. Valot, B. Pasquet, Appl. Surf. Sci. 252 (2006) 7048.
[4] J.C. Martz, D.W. Hess, J.M. Haschke, J.W. Ward, B.F. Flamm, J. Nucl. Mater 182 (1991) 277.
[5] X. Yang, M. Moravej, S.E. Babayan, G.R. Nowling, R.F. Hicks, J. Nucl. Mater. 324 (2004) 134.
[6] J.M. Veilleux, M.S. El-Genk, E.P. Chamberlin, C. Munson, J. FitzPatrick, J. Nucl. Mater 277 (2000) 315.
[7] S. Sinha, E. Ramadasan, V.P. Jathar, K. Dasgupta, K.C. Sahoo, L.M. Gantayet, Appl. Surf. Sci. 253 (2007) 4404.
[8] D. Bauerle, Laser Processing and Chemistry, third ed., Springer-Verlag, Berlin, 2000.
[9] P.R. Willmott, J.R. Huber, Rev. Mod. Phys. 72 (2000) 315.
[10] J. Steinbeck, G. Braunstein, M.S. Dresselhaus, T. Venkatesan, D.C. Jacobson, J. Appl. Phys. 58 (1985) 4374.
[11] J.R. Ho, C.P. Grigoropoulos, J.A.C. Humphrey, J. Appl. Phys. 78 (1995) 4696.
[12] J.H. Yoo, S.H. Jeong, X.L. Mao, R. Greif, R.E. Russo, Appl. Phys. Lett. 76 (2000) 783.
[13] A. Bogaerts, Z. Chen, R. Gijbels, A. Vertes, Spectrochim Acta, Part B 58 (2003) 1867.
[14] V. Oliveira, R. Vilar, Appl. Surf. Sci. 253 (2007) 7810.
[15] A. Bogaerts, Z. Chen, J. Anal. Atom. Spectrom. 19 (2004) 1169.
[16] R. Kelly, A. Miotello, Nucl. Instrum. & Methods in Phys. Res. B 122 (1997) 374.
[17] A.V. Gusarov, I. Smurov, J. Phys. D: Appl. Phys. 36 (2003) 2962.
[18] A. Miotello, R. Kelly, Appl. Phys. A 69 (1999) S67.
[19] M. Von Allmen, Laser Beam Interactions with Materials, Springer, Heidelberg, 1987.
[20] B.N. Chichkov, C. Momma, S. Nolte, F. von Alvensleben, A. Tunnermann, Appl. Phys. A 63 (1996) 109.
[21] R. Kelly, A. Miotello, Appl. Surf. Sci. 96–98 (1996) 205.
[22] M.M. Martynyuk, Sov. Phys. Tech. Phys. 21 (1976) 793.
[23] N.M. Bulgakova, A.V. Bulgakov, Appl. Phys. A 73 (2001) 199.
[24] S.A. Mahmoud, Solid State Sci. 4 (2002) 221.
[25] FACT-Factsage 5.00 compound database, March, 2001.
[26] R. Kelly, J. Chem. Phys. 92 (1990) 5047.
[27] C.T. Walters, A.H. Clauer, Appl. Phys. Lett. 33 (1978) 713.
[28] I. Barin, O. Knacke, Thermochemical Properties of Inorganic Substances, Springer-Verlag, Berlin, 1977.
[29] W.R. Evans, D.D. Allred, Thin Solid Films 515 (2006) 847.
[30] H.M. Liddell, J. Phys. D: Appl. Phys. 7 (1974) 1588.